ISSN 2348-375X

Unique Journal of Engineering and Advanced Sciences

Available online: www.ujconline.net

Research Article

IMAGE DENOISING BASED ON SYMMETRICAL FRACTIONAL OVERCOMPLETE WAVELET TRANSFORM

Aiswarya K[1*], Jayaraj V[2]

[1]Student, M.E. Communication systems Nehru Institute of Engineering and Technology, Coimbatore, India
[2]Professor, ECE Nehru Institute of Engineering and Technology, Coimbatore, India

Received: 29-12-2013; Revised: 27-01-2014; Accepted: 25-02-2014

*Corresponding Author: **Aiswarya. K**
Student, M.E.Communication systems Nehru Institute of Engineering and Technology,Coimbatore Email:aiswaryaachu9197@gmail.com

ABSTRACT

A fractional overcomplete wavelet transform's filter banks, which are half symmetrical, approximately shift-invariant and minimum-even-length is designed and constructed. A novel designing scheme for the symmetrical and minimum-even-length low-pass filter bank is proposed. High-pass filter banks with approximately shift-invariant property are constructed through Toeplitz matrix factorization, which is easier than the existing methods. This type of wavelet is expected to provide favourable conditions to image denoising. Fractional overcomplete wavelet transform gives better denoising than existing wavelets including orthogonal compact support dyadic wavelet and orthogonal symmetrical M-band wavelet system.

Keywords: Overcomplete wavelet transform, Filter banks,

INTRODUCTION

Image denoising based on wavelet transforms is impressive for the last several decades. However, modelling statics of pixels position distribution in natural images is more difficult than that of the wavelet coefficient[1,2]. In addition, the effectiveness of image denoising using wavelet transform is restricted by not only the the scheme of denoising and different types of images, but the properties of wavelet itself. The property of wavelet is one of the most important factors for image denoising such as the vanishing moments, regularity, symmetry, compact support, directional selection, orthogonality, shift-invariance and the resolution of frequency and space properties, and etc.

These properties of wavelet have a strong impact on the decomposition and reconstruction of image in many ways, such as the statistical distribution of wavelet coefficients, which will influence the validity of image denoising. For example, spare representation of image by wavelet is under control by the number of the vanishing moments, also by the regularity and the compact support properties. But the symmetry of wavelet corresponds to the linear phase of wavelet filters, is able to effectively suppress the aliasing error. The linear irregularity which is the edge in image can be optimal spare represented by wavelet system having more directional selections. However, the loss of shift-invariance, which is characterized by the critically decimated wavelet transforms, will seriously result in wavelet coefficients different due to the signal shift. This always brings in new reconstructing image errors and artifacts. Last but not least, higher resolution of frequency and space properties can be used to analyze image frequency information more accurately. Unfortunately, there is no such wavelet transform which has all of the preceding properties because of more restrictions during the wavelet construction.

In addition, redundant information from MRA is also a very important factor for image denoising, since they are able to offer us more flexibility to design denoising schemes[3]. For example, we can use the redundant coefficients to replenish the missing coefficients introduced by the thresholding during denoising. However, the coefficients for the orthonormal system are not redundant; but this is not the case for overcomplete wavelets(or frames). In other words, the available coefficients contain the information of the missing coefficients if the system is redundant.

The overcomplete wavelets (or wavelet frames) can be constructed to be with symmetrical, approximately shift-invariant and with higher vanishing moments, which means more designing flexibility than critically sampled DWTs. In addition, overcomplete wavelets provide more controlled redundant information than critically sampled DWTs and also are characterized with denser time-frequency lattices. More theories about overcomplete wavelets and its applications can be referred to literatures[3-8] and references therein for more details.

In this paper, we propose an approach to construct the fractional overcomplete wavelet system with symmetrical scaling filter (low-pass filter) and with minimum even-length compact support. This wavelet system has higher vanishing moments and is approximately shift-invariant. The construction of symmetrical scaling filter is given by a theory. Meanwhile, a more simple algorithm by Toeplitz matrix spectral factorization for obtaining high-pass filter is also given. The constructing examples show that this algorithm is easier than the method in[9] and has lower computational complexity. Finally, these wavelet filter banks are used to image denoising; the denoising results comparing to dyadic wavelet system and M−band wavelet system show a good effect.

Fractional overcomplete discrete wavelet transforms

The double density DWT[7] and the higher density DWT[8], which are approximately shift-invariant and with denser time-frequency resolution, are two distinct overcomplete wavelet transforms. The double density DWT, which has twice redundancy, is a compromise thought between the critically sampled DWT and the undecimated DWT. Higher density DWT like the double density DWT provides a higher sampling in both time and frequency. Meanwhile, it transforms the signal of N discrete points into M points of the wavelet coefficients, where M>N. Therefore, the wavelet coefficients have more redundant information than those in the original signal via higher density DWT.

The fractional DWT[10] as an improvement to orthogonal critically sampled DWT, can divide the band of signal more finely than M-Band (M≥2) DWT. Thus, it has a better resolution in frequency domain, but with lower time resolution and doesn't have the shift-invariance property. In literature[11], a design scheme for fractional DWT filter banks was proposed using the iterative method. It was also pointed out that when the regularity (smoothness) of fractional wavelet function increases, the error caused by shifting can be arbitrarily small and thus is approximately shift invariant. Fractional overcomplete DWT with approximate shift-invariance property was proposed in literature[12]. Based on the works[7-12], the characteristics of fractional overcomplete wavelet transforms were summarized in[9] and a constructing method for the low-pass and high-pass of FOWT filter banks was proposed. However, the designed low-pass filter banks therein do not have symmetrical property. What's more, the construction of the high-pass filter is trivial and computationally intensive.

Let $\sqrt{a}\Psi(at-b)$ be the wavelet function of the dilation a and translation b version of wavelet function ψ(t). The discrete wavelet function can be obtained by discretizing a, b as $\{2^n, k\}_{n,k\varepsilon Z}$. However, such discrete wavelet is shift-variant and also has a lower constant Q−factor. Suppose that the dilation and translation factor a, b are discretized as $\{q^n/p^n, spk/q\}_{n,k\varepsilon Z}$, wherein p,q,s are positive integers. After the discretization, the dilation factor becoming q^n/p^n and the redundancy is given by $\frac{1}{s}\frac{1}{q/p-1}$. Hence such a wavelet is fractional dilation and overcomplete. Like the case in paper [9], we set q =3, p=2,s= 1, and thus denoting it is 3/2 dilation overcomplete wavelet transform. The analogous designing method in the following can be applied to other fractional dilation factors as well.

The ideal 3/2 dilation overcomplete wavelet transform filter bank is illustrated in Fig 1.

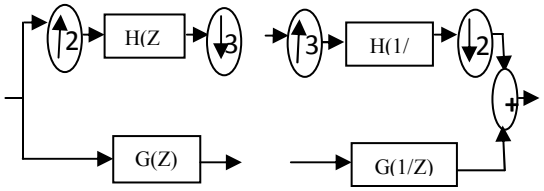

Figure 1:Ideal 3/2 Overcomplete Filter Bank

From literature [9], we have perfect reconstruction (PR) conditions of the filter bank in Fig.1.

$H(z^{-1})\,H(z) + H(-z^{-1})H(-z) + 6G(z^2)G(z^{-2}) = 6$ (1)

$H(z^{-1})\,H(Wz) + H(-z^{-1})\,H(-Wz) = 0$ (2)

$H(z^{-1})H(W^2z) + H(-z^{-1})H(-W^2z) = 0$ (3)

Where $W = e^{-2\pi/3}$.

We can see that the low-pass filter is 3/2 sampled, while the high-pass filter has the same rate as input signal. Thus, this kind of filter bank is partially shift-invariant for only the high-pass filter is shift-invariant. We call it "ideal" because this filter bank can't satisfy PR conditions using FIR filters, i.e. Eq. (1),(2),(3) are not tenable except for an insignificant special solution. Therefore, we must forge them into Fig.2 since we need FIR solutions [9]. Note that the high-pass filter G(z) in Fig.1 can be separated into three new high-pass filters $G_i(z)$,(i=0,1,2). They have 3-times down-sampling rate if they satisfy the following equation

$g_0(n-2) = g_1(n-1) = g_2(n)$ (4)

where $g_i(n)$, (i =0,1,2) is the impulse response of $G_i(z)$, (i =0,1,2). Then the filter bank showed in Fig.1 is essentially the same as the one in Fig.2, thus it also doesn't have FIR PR solutions. However, they are not equivalent, and we can obtain approximate solutions using FIR filters in Fig.2. From the literature [9], the PR conditions of the filter bank in Fig.2 is expressed as following

$$H(Z)H(1/Z)+H(-Z)H(-1/Z)+2\sum_{i=0}^{2} G_i(Z^2)G_i(1/Z^2)=6 \quad (5)$$

$$H(WZ)H(1/Z)+H(-WZ)H(-1/Z)+2\sum_{i=0}^{2} G_i(W^2Z^2)G_i(1/Z^2)=0 \quad (6)$$

$$H(W^2Z)H(1/Z)+H(-W^2Z)H(-1/Z)+2\sum_{i=0}^{2} G_i(WZ^2)G_i(1/Z^2)=0 \quad (7)$$

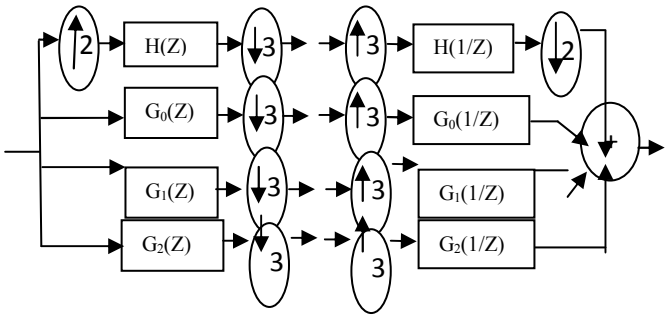

Figure 2: 3/2 Overcomplete Filter Bank. Less Constrained than those in Fig.1.

Construction of symmetrical low-pass filter with minimum-length

The discrete polynomial signal, which processed by the low-pass filter H(z) in Fig.2, should normally be able to retain the N−1 order part of the discrete polynomial. The high-pass filters $G_i(z)$ (i=0,1,2) should be able to eliminate the K_i order part of the discrete polynomial signal. Noting that, for the critically sampled orthogonal wavelet system, we have $N=K_i$ in general. For fractional overcomplete wavelet systems, however, it is usually required $N \geq K_i$ in order to obtain higher order vanishing moments or to get a more smooth wavelet function. The following examples show that the larger K_i with the identical N indicates less smooth scaling functions. Based on assumption and the multi-resolution analysis (MRA) theory, it can be seen from Fig.2 that the low-pass filter can be written as the form in the following lemma.

Lemma 1

The structure of low-pass filter H(z) and high-pass filter $G_i(z)$ in Fig. 2 is given as following

$$H(Z)=(1+Z^{-1})^N (1+Z^{-1}+Z^{-2})^N Q(Z) \quad (8)$$

$$G_i(Z)=(1-Z^{-1})^{K_i} V_i(Z), i=0,1,2 \quad (9)$$

where N is the number of zero point of low-pass filter at z = −1, $z = e^{i2\pi/3}$ and $z = e^{i4\pi/3}$, K_i(i = 0, 1, 2) is the number of zero point of high-pass filter at z = 1, and $N \geq K_i$, $(1 + z^{-1})(1 + z^{-1} + z^{-2})$ XQ(z). Noting that K_i (i = 0, 1, 2) can be different in Eq(9), but we generally assume that they are equal. It is known that the conditions below for the length of low-pass filter should be satisfied if one is going to attain low-pass filter with minimum-length[12].

Lemma 2

The degree of low-pass filter polynomial H(z) in Fig.2 should satisfy $LH \geq 3N+2K-1$ (10)

where $K = \min(K_0, K_1, K_2)$.

Imposed on the low-pass filter $H(z)$ with minimum-length and linear phase(or symmetrical) property, it is known by Lemma 2 that the factor $Q(z)$ in Eq.(8) should be symmetric and its length shorter than

$2K - 1$. That is, the length of the lowpass filter h(n) should be at least as long as $3N + 2K - 1$. Thereby, the shortest support length of the low-pass filter h(n) in 3⁄2 overcomplete wavelet transforms is

$3N + 2K - 1$. Specifically, we just consider the situation of L_H is the least even number larger than $3N + 2K - 1$. The designing scheme for 3⁄2 overcomplete low-pass filter with minimum-evenlength and symmetrical properties is proposed in the following theorem.

Theorem 1

Given the parameter N,K in Eq.(7) and let $N \geq K$, then the shiftinvariant symmetrical fractional overcomplete wavelet low-pass filter with minimumlength can be written as

$$H(Z)=Z^{-(K-1)}\sqrt{6}\left(\frac{1+Z^{-1}}{2}\right)^N X \sum_{p=0}^{K-1}\sum_{q=0}^{p}\binom{N}{q+\frac{N}{2}-1}\binom{p-q+N-1}{N-1}\left(\frac{4}{3}\right)^{p-q}\left(\frac{-Z^{-1}+2-Z}{4}\right)^p \quad (11)$$

With N is odd

$$H(Z)=Z^{-(K-1)}\sqrt{6}\left(\frac{1+Z^{-1}}{2}\right)^{N+1}\left(\frac{1+z^{-1}+z^{-2}}{3}\right)^N X \sum_{p=0}^{K-1}\sum_{q=0}^{p}\binom{q+\frac{N}{2}-\frac{1}{2}}{\frac{N}{2}-\frac{1}{2}}\binom{p-q+N-1}{N-1}\left(\frac{4}{3}\right)^{p-q}\left(\frac{-Z^{-1}+2-Z}{4}\right)^p \quad (12)$$

Proof 1

We just consider situation of N is odd, the same as the case N is even. Supposing low-pass filter H(z) is symmetric and its impulse response h(n) is L−length, which $L \geq 3N + 2K - 1$. Then H(z) can be represented as the polynomial of ω by setting $z=e^{i\omega}$. Let $z=e^{i\omega}$, we have

$$x = \frac{1}{4}(-Z^{-1}+2-Z) = \sin^2\frac{\omega}{2} = \frac{1}{2}(1-\cos\omega) \quad (13)$$

Then

$$1-\frac{4}{3}x = \frac{1}{3}(Z^{-1}+1+Z) = \frac{1}{3}z(1+z^{-1}+z^{-2}) \quad (14)$$

$$1-x = \frac{1}{4}(Z^{-1}+2+Z) = \cos^2\frac{\omega}{2} \quad (15)$$

The factor $(1 + z^{-1})$ of Eq.(8) can be expressed by x as follows

$$M_{01}(\omega) = 2\cos\frac{\omega}{2} = 2\sqrt{1-x} \quad (16)$$

After one delay shift, the factor $(1+z^{-1}+z^{-2})$ of Eq.(8) can be expressed as follows

$$M_{02}(\omega) = (z^{-1}+1+z) = 4\left(\frac{3}{4}-x\right) \quad (17)$$

Noting that if H(z) is symmetric, then the factor Q(z) is also symmetric. Thus, it can also be expressed by x, denoting it to be A(x), then Eq.(8) can be written as

$$T(x) = (1-x)^{N/2}\left(\frac{3}{4}-x\right)^N A(x) \quad (18)$$

By Eq.(13), it is easily seen that $z = 1,-1, \frac{1}{2} \pm \frac{\sqrt{3}}{2}i$ of corresponds to x = 0, 1, ¾ of Eq.(18) respectively. That means the property of H(z) at

$z = 1,-1, \frac{1}{2} \pm \frac{\sqrt{3}}{2}i$ indicates the same property of T(x) at x = 0,1,3/4 . Then, we obtain the following identities

$T(0) = 1;$

$T^{(i)}(0) = 0, (i = 1\ldots\ldots K-1);$

$T^{(i)}(1) = 0, (i = 0\ldots\ldots N/2-1);$

$T^{(i)}(3/4) = 0, (i = 0\ldots\ldots N-1).$

Taking into account flatness at z = 1 of H(z), that is flatness at x = 0 of T(x), then T(x) should have the following representation by Lemma 1

$$1-T(x) = B(x)x^K \quad (19)$$

$$(1-x)^{N/2}\left(\frac{3}{4}-x\right)^N A(x) + B(x)x^K = 1 \quad (20)$$

That is

$$A(x) = \frac{1-B(x)x^K}{(1-x)^{N/2}\left(\frac{3}{4}-x\right)^N} \quad (21)$$

Then A(x) can be obtained by the following truncated Taylor series

$$\frac{1}{(1-x)^{N/2}\left(\frac{3}{4}-x\right)^{N}}=A(x)+O(|x|^{K}) \qquad (22)$$

where

$$\frac{1}{(1-x)^{N}}=\sum_{n=0}^{\infty}\binom{n+N-1}{N-1}x^{n}$$

$$\frac{1}{\left(\frac{3}{4}-x\right)^{N}}=\sum_{n=0}^{\infty}\left(\frac{4}{3}\right)^{N}\binom{n+N-1}{N-1}\left(\frac{4}{3}\right)^{n}x^{n}$$

Are the Taylor series of $\frac{1}{(1-x)^{N}}$ and $\frac{1}{(3/4-x)^{N}}$ respectively. That is A(x) is the Taylor polynomial resulting from expanding expression Eq.(22) around x=0 and keeps only the first K terms. From Eq.(22), the polynomial T(x) is expressed by standardization ($H(1)=\sqrt{6}$)

$$T(x)=\sqrt{6}(1-x)^{\frac{N}{2}}\left(\frac{3}{4}-x\right)^{N}X\sum_{p=0}^{K-1}\sum_{q=0}^{p}\left(\frac{4}{3}\right)^{N}\binom{q+\frac{N}{2}-1}{\frac{N}{2}-1}\binom{p-q+N-1}{N-1}\left(\frac{4}{3}\right)^{p-q}x^{p}=$$

$$\sqrt{6}(1-x)^{N/2}\left(1-\frac{4}{3}x\right)^{N}\binom{q+\frac{N}{2}-1}{\frac{N}{2}-1}\binom{p-q+N-1}{N-1}\left(\frac{4}{3}\right)^{p-q}x^{p} \qquad (23)$$

Substituting x into (23), then Eq.(11) is obtained.

Remark 1

It should be noted that the proof of Theorem 1 doesn't particularly point out the parity of the parameter N. In fact, we can see from Eq.(11) and Eq.(12) that N can be either odd or even. Thus, the length of low-pass filter h(n) is even-length and the factor $z^{-(K-1)}$) of Eq.(11) and Eq.(12) is used to adjust the shift from the construction.

Example 1:

LetN=3,K= 1, the minimum-length of low-pass filter should be 10. From Theorem 1, we have

$$H(Z)=\sqrt{6}\left(\frac{1+Z^{-1}}{3}\right)^{3}\left(\frac{1+Z^{-1}+Z^{-2}}{3}\right)^{3}$$, which is

identical to literature[9]. The impulse response is shown in Table 1, and the corresponding scaling function φ(t) from the iterated low-pass filter h(n) seen in Fig.3.

Example 2:

LetN=3,K= 2, the minimum-length of low-pass filter should be 12. From Theorem 1, we have

$$H(Z)=\frac{\sqrt{6}}{8}\left(\frac{1+Z^{-1}}{2}\right)^{3}\left(\frac{1+Z^{-1}+Z^{-2}}{3}\right)^{3}\left(-11Z^{-2}+30Z^{-1}-11\right)$$

The impulse response is shown in Table 1; the scaling function φ(t) is illustrated in Fig.3 is less smooth than the case in example 1 for the higher parameter K

Example 3:

LetN=4,K= 2, the minimum-length of low-pass filter should be 16. From Theorem 1, we have

$$H(Z)=\frac{\sqrt{6}}{24}\left(\frac{1+Z^{-1}}{2}\right)^{4}\left(\frac{1+Z^{-1}+Z^{-2}}{3}\right)^{4}\left(-47Z^{-2}+118Z^{-1}-47\right)$$

The impulse response shown in Table 1; the scaling function φ(t) illustrated in Fig.3 . It is necessary to point out that there exists the odd-length solution for this case which is not shown in Table1, that is

$$H(Z)=\frac{\sqrt{6}}{6}\left(\frac{1+Z^{-1}}{2}\right)^{4}\left(\frac{1+Z^{-1}+Z^{-2}}{3}\right)^{4}\left(-11Z^{-2}+28Z^{-1}-11\right)$$

Construction of high -pass filters

In this section, we are going to complete the filter bank illustrated in Fig.2 using the low-pass filter $H(z)$ constructed above. In this case, the low-pass branch need to be modified because we can not straightly obtain the high-pass filters $G_i(z)$ by some approaches like matrix spectral factorization if the sampling rate is fractional. Consequently, we need convert the low-pass branch in Fig.2 into integer sampling rate using the polyphase representation $H(z) = H_0(z^2) + z^{-3}H_1(z^2)$ like the Fig. 9 in literature [13]. This type of polyphase representation of $H(z)$ is available by the Type II polyphase representation of $H(z)$ as

$H(z)=R_1(z^2)+z^{-1}R_0(z^2)$ (24)

So $H(z) = R_1(z^2)+z^{-3}z^2R_0(z^2)$ (25)

Therefore, denoting $H_0(z) = R_1(z)$ and

$H_1(z) = zR_0(z)$, then we have

$H(z)=H_0(z^2)+z^{-3}H_1(z^2)$ (26)

This representation of $H(z)$ converts the low-pass branch of Fig.2 into two branches, where decimated three after the $H_0(z)$ and $H_1(z)$ like the high pass branches. In order to use the PR condition Eq.(5),(6),(7), it is needed to rewrite the filter bank of Fig.2 into its polyphase matrix representation. Type I polyphase representation of low-pass branch $H_0(z)$ is represented as following

$H_0(z)=H_{00}(z^3)+z^{-1}H_{01}(z^3)+z^{-2}H_{02}(z^3)$ (27)

The filters $H1(z)$ and $Gi(z)$ are also written by their Type I polyphase representation. By the perfect reconstruction condition presented above, we get the following identical equation through the polyphase matrix representation.

$$\begin{bmatrix} H^{T}(1/Z) & G^{T}(1/Z) \end{bmatrix}\begin{bmatrix} H(Z) \\ G(Z) \end{bmatrix}=I_3 \qquad (28)$$

Where

$$H(Z)=\begin{bmatrix} H_{00}(Z) & H_{01}(Z) & H_{02}(Z) \\ H_{10}(Z) & H_{11}(Z) & H_{12}(Z) \end{bmatrix}$$

$$G(Z)=\begin{pmatrix} G_{00}(Z) & G_{01}(Z) & G_{02}(Z) \\ G_{10}(Z) & G_{11}(Z) & G_{12}(Z) \\ G_{20}(Z) & G_{21}(Z) & G_{22}(Z) \end{pmatrix}$$

Then, by Eq.(28), we have

$$G^{T}(1/Z)G^{T}(Z)=I_3-H^{T}(1/Z)H^{T}(Z) \qquad (29)$$

Unfortunately, it is to be noticed that the polyphase structures of high pass representation fail to exploit the coefficient symmetry in the case of a linear-phase FIR low-pass filter $H(z)$ constructed above. This point has been verified from example($N = 3, K = 1$) in literature [9], where the high-pass pass filters are asymmetrical even though the low-pass filter is symmetrical. Thus, the highpass filters $G_i(z)$ constructed in this section are not symmetrical although the corresponding $H(z)$ is symmetrical

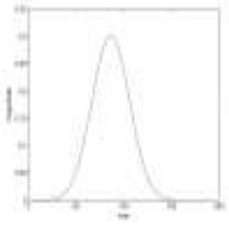

(a) scaling function ϕ(t) of Example 1

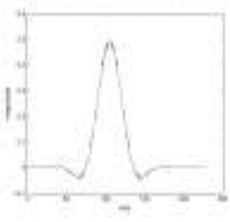

(b) Scaling Function ϕ(t) of Example 2

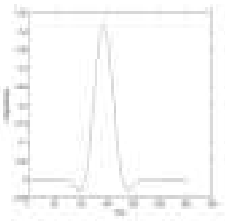

(c) scaling function ϕ(t) of Example 3

Figure 3: Symmetrical Scaling Function of Overcomplete Fractional Wavelet

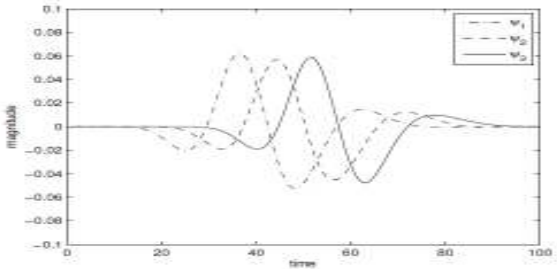

Figure 4a: Wavelet Function Ψ(t) with N=3 ,K=1

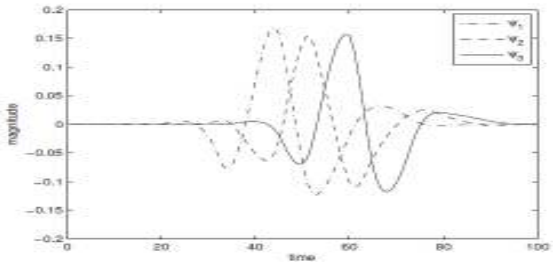

Figure 4b: Wavelet Function Ψ(t) with N=3 ,K=2

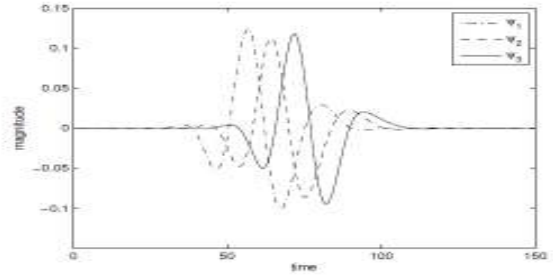

Figure 4c: Wavelet Function Ψ(t) with N=4 ,K=2

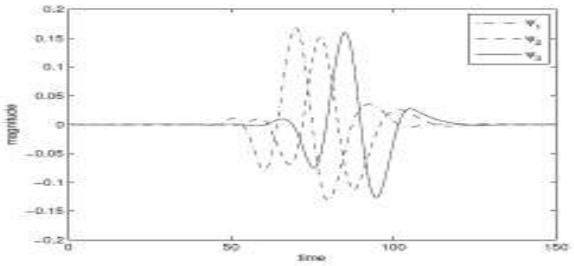

Figure 4d: Wavelet Function Ψ(t) with N=5 ,K=3

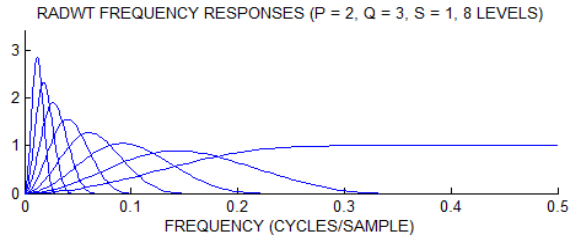

Figure 4e: RADWT Frequency Responses

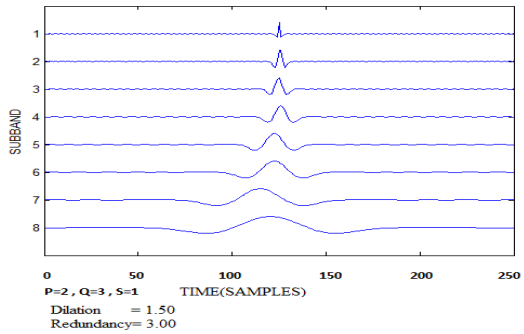

Figure 4f: Wavelet at Several Scales

Now, we are going to obtain G(z) in Eq.(29) by matrix spectral factorization. A variety of approaches have been designed to solve the matrix spectral factorization. The algorithm to obtain G(z) in literature[9] is symmetric factor extraction, which has great computational complexity and need extra computation to adjust the high pass filters to satisfy the shift-invariant property.

However, we find that in this paper the associated high-pass filters $G_i(z)$ can be obtained directly by the Toeplitz matrix decomposition. This decomposition is simpler than symmetric factor extraction used in paper[9] and the approximately shift-invariant property of high-pass filters is also satisfied, which means no need additional adjusting. Substituting the low pass filter from literature[9] with[1] N=3,K=1;(2)N=4,K= 2 in to Eq.(29), after iterating 3000 times of Toeplitz matrix decomposition, we obtain almost the same result as in that paper (see Table 2 and Table 3).We also obtain the PR and approximately shift-invariant high-pass filters on the basis of the symmetrical low-pass filter obtained in section 3 after iterating 3000 times via Toeplitz matrix decomposition. The high-pass filter coefficients associated to symmetrical low-pass filter in example 2, 3 shown in Table 4 and Table 5 respectively. As pointed in paper[11] the amount of wavelet functions is increased with the scale level j becoming higher. In other words, there is no unique wavelet function at fixed

level scale j, which is totally different from the M−band wavelet case. Actually, there exists 2^{j-1} wavelet function at level j for each high-pass filter $g_i(n)$[9]. One of the corresponding wavelet functions satisfying approximately shift invariant properties is illustrated in Fig.4.

Image denoising with overcomplete fractional wavelet

In order to evaluate the overcomplete fractional wavelet system constructed above, we are going to discuss its application in image denoising in this section. Its special properties, including higher vanishing moments, redundant coefficients representation, approximate shift-invariant, partly linear phase (only scaling function is symmetrical) and with more direction selectivities (16 subbands after one scale decomposition), are expected to provide favourable conditions to image denoising. In order to fully analyze the denoising effects which result from these properties, we compare the denoising performance to other wavelet systems including orthogonal compact support dyadic wavelet and the orthogonal symmetrical M−band wavelet system. For the dyadic wavelet transform, we use the orthogonal compact support Daubechies wavelet with higher vanishing moments but asymmetrical. For M−band wavelet transform, we use the 3-band wavelet system[14] which is symmetrical, orthogonal compactly supported. For the overcomplete fractional wavelet transform, we use the asymmetrical and the partly symmetrical overcomplete fractional wavelet with N=4,K= 2 respectively constructed above. It should be noticed that the overcomplete fractional wavelet system is redundant, approximately shift-invariant and with more directional selectivities. In addition, it has partly linear phase for symmetrical overcomplete fractional wavelet.

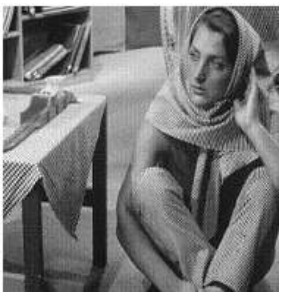

(a) Barbara image with textures has obviously directional

(b) Crowd image with more details

(c) Barbara degraded by Gaussian noise with σ =0.02

(d) Crowd degraded by Gaussian noise with σ=0.02

Figure 5: The Original Images and the Noisy Images Degraded By Gaussian Noise with σ=0.02

We also use two standard images "crowd.jpg" and "barbara.jpg" degraded by Gaussian noise with σ=0.02 as the pending processed object images shown in Fig. 5. The crowd image has more details, however, the textures of barbara image have obvious directions. We expect that overcomplete fractional wavelet system can be used to deal with those images more powerful. For denoising scheme, we just adopt soft thresholding denoising algorithm based on wavelet coefficients, which with the threshold parameters changing from 0.08 to 0.8. This is because the key points in this paper we are going to emphasize is not the denoising algorithm designing. The PSNR(Peak Signal to noise Ratio) and NMSE(Normalized Mean Square Error) are taken as the objective evaluation criterion of image denoising. In addition, we also take subjective evaluation as one of criterion to evaluate the effect of image deonising.

The denoising results corresponding to thresholding 0.8 are illustrated in Fig.6 and Fig.8 associated with barbara and crowd image respectively. Other outcomes of different thresholds are not shown here because of the analogous effect. From the subjective visual effective, it can be easily seen that overcomplete fractional wavelet has better performance than other wavelet systems no matter for the Barbara or crowd image. Especially, for the 3-band wavelet system, the denoising effect is very poor even though it is linear phase filter system. For the dyadic wavelet, it also can be seen that there are some obvious undesirable artifacts, which can not be completely eliminated even by other Daubenchies wavelet system with higher vanishing moments. Finally, for the symmetrical overcomplete fractional wavelet, it can be seen from Fig.6(d) and Fig.8(d) that there is a little bit superiority than that of asymmetrical overcomplete fractional wavelet shown in Fig.6(c) and Fig.8(c).

When the the threshold is lower, from the PSNR view, 3-band wavelet shows good performance seen in Fig.7(a) and Fig.9(a) even though the subjective visual facts are not like that, followed by the dyadic wavelet system and the last is overcomplete fractional wavelet, where the symmetrical system is a little bit better than asymmetrical case. However, if the threshold becomes higher, the PSNR value of 3-band wavelet system decays faster than other wavelet systems, and overcomple fractional wavelet system maintains relatively stable. In the NMSE case, it can be found analogous results shown in Fig.7(b) and Fig.9(b). In particular, the symmetrical fractional overcomplete wavelet system obviously keep better the performance than other wavelet systems when the threshold becomes higher.

In summary, the 3-band wavelet performance is good if the threshold is lower from objective visual point. However, it should be pointed out that the lower threshold means weakly denoising effects. When the thresholding becomes higher, the symmetrical fractional overcomplete wavelet system maintains good performance whether it is from the subjective or objective perspective. The reasons can be interpreted in its redundant representation, higher vanishing moments, partly linear phase and approximately shift-invariant property.

(a) Denoising image by DB3

(b)Denoising image by3-band wavelet

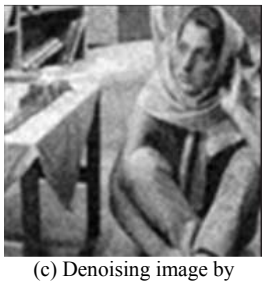

(c) Denoising image by OFWT

(d)Denoising image by symmetrical OFWT

Figure 6: Denoising Barbara Image by Different Wavelets with the Threshold Set to 0.8

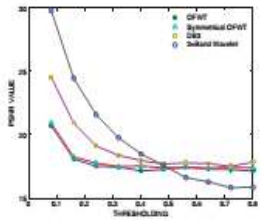

(a)The PSNR variation trend of different wavelets according to thresholding

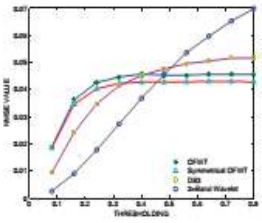

(b) The NMSE variation trend of different wavelets according to thresholding

Figure 7: The PSNR and NMSE Variation of Barbara Image According to Different Thresholding Denoising by the Different Wavelets

(a) Denoising image by DB3

(b)Denoising image by3-band wavelet

(c) Denoising image by OFWT

(d)Denoising image y symmetrical OFWT

Figure 8: Denoising Crowd Image by Different Wavelets with the Threshold Set to 0.8

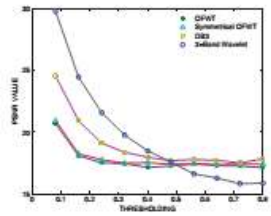

(a)The PSNR variation trend of different wavelets according to thresholding

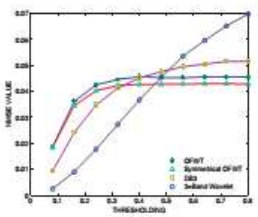

(b) The NMSE variation trend of different wavelets according to thresholding

Figure 9: The PSNR and NMSE Variation of Crowd Image According to Different Thresholding Denoising by the Different Wavelets

CONCLUSION

Symmetrical fractional overcomplete wavelet transforms is implemented and constructed here . The construction scheme of the 3/2 overcomplete low-pass filter with symmetrical and minimum-even-length properties is also proposed and a simple designing scheme for the construction of the high-pass filter which satisfies approximately shift-invariant property is developed. This proposed scheme only need Toeplitz matrix spectral factorization which means more iteration, for example 3000. Thus this method requires the computer should have higher computer memory and higher computing speed. Eventhough the scheme having so many benefits , we cannot get the symmetrical high-pass filter banks . In order to evaluate the overcomplete fractional wavelet system constructed above, check it in the area of image denoising . Its special properties, including higher vanishing moments, redundant coefficients representation, approximate shift-invariant, partly linear phase (only scaling function is symmetrical) and with more direction selectivities (16 subbands after one scale decomposition), are expected to provide favorable conditions to image denoising. In order to fully analyze the denoising effects which result from these properties, we compare the denoising performance to other wavelet systems including orthogonal compact support dyadic wavelet and the orthogonal symmetrical $M-$band wavelet system.

REFERENCES

1. Portilla J, Strela V, Wainwright MJ, Simoncelli EP. Image denoising using scale mixtures of gaussians in the wavelet domain, IEEE Trans.on Image Processing.2003; 12 (11): 1338.
2. Miller M, Kingsbury N. Image denoising using derotated complex wavelet coefficients., IEEE Trans. on Signal Processing.2008; 17(9): 1500.
3. Shen Z. Wavelet frames and image restorations, in: Proceedings of the International Congress of Mathematicians, Vol. IV, Hyderabad, India. 2010; 2834.
4. Frazier M, Garrig G, Wang K, Weiss G. A characterization of functions that generate wavelet and related expansion, J. Fourier Analysis Appl. 1997; 3(1): 883.

5. Bownik M. A characterization of affine dual frames in l2(rn), Appl. Comput. Harmonic Anal. 2000; 8(2): 203.
6. Han B. On dual wavelet tight frames, Appl. Comput. Harmonic Anal. 1997; 4(4): 380.
7. Selesnick IW. The double density dwt, in: Wavelets in Signal and Image Analysis: From Theory to Practice, A. Petrosian and FG. Meyer, Eds. Norwell, MA: Kluwer. 2001.
8. Selesnick IW. A higher density discrete wavelet transform, IEEE Trans. On Signal Processing. 2006; 54(8): 3039.
9. Bayram I, Selesnick IW.Overcomplete discrete wavelet transforms with rational dilation factors, IEEE Trans. on Signal Processing.2009; 5 (1): 131.
10. Auscher P. Wavelet bases forl2(r)with rational dilation factor, in: MB. Ruskai,editor,Wavelets and Their Applications, Jones and Barlett, Boston. 1992; 439.
11. Blu T. Iterated filter banks with rational rate changes connection with discrete wavelet transforms, IEEE Trans. on Signal Processing. 1993; 41(12): 3232.
12. Bayram I, Selesnick IW. Design of orthonormal and overcomplete wavelet transforms based on rational sampling factors, in: Wavelet Applications in Industrial Processing V Proceedings of SPIE.2007; 6763: 1.
13. Abdelnour AF, Selesnick IW. Symmetric nearly shift-invariant tight frame wavelets, IEEE Trans. on Signal Processing. 2005; 53(1): 231.
14. Chui CK, Lian JA.Construction of compactly supported symmetric and antisymmetric orthonormal wavelets with scale3, Appl. Comput. Harmonic Anal. 1995; 2: 21.

Table 1: The Coefficients of Symmetrical and Minimum-Even-Length Low-Pass Filter

N = 3, K =1	N = 3,K =2	N = 4,K = 2	N = 5,K = 3
0.011340	-0.01559	-0.00185	0.000939
0.068041	-.05103	-0.01200	0.004913
0.204124	-0.04110	-0.03406	0.009568
0.396908	0.12616	-0.04547	0.000496
0.544331	0.45927	0.01338	-0.03745
	0.74703	0.19357	-0.07973
		0.45557	-0.04111
		0.65560	0.158941
			0.478415
			0.729773

Table 2: High-Pass Filter Coefficients Satisfying Approximately Shift-Invariant Property, with N = 3, K = 1 Obtained by Toeplitz Matrix Decomposition

$g_0(n)$	$g_1(n)$	$g_2(n)$
0.649214	0	0
-0.48258	0.63774	0
-0.15058	-0.46683	0.64524
-0.01477	-0.14814	-0.49094
-0.00118	-0.02267	-0.13148
0	0	-0.02152
0	0	-0.00119

Table 3: High-Pass Filter Coefficients Satisfying Approximately Shift-Invariant Property with N = 4, K = 2 Obtained by Toeplitz Matrix Decomposition

$g_0(n)$	$g_1(n)$	$g_2(n)$
-0.4091774	0	0
0.6087859	-0.4186841	0
-0.0417616	0.6376358	-0.4172096
-0.1102300	-0.06594183	0.6195211
-0.0440127	-0.1122649	-0.0319971
-0.0034016	-0.0350639	-0.1308184
-0.0002024	-0.0056809	-0.0349423
0	0	-0.0043211
0	0	-0.0002324

Table 4: High-Pass Filters Coefficients Satisfying Approximately Shift-Invariant Properties with N = 3, K = 2 by Toeplitz Matrix Decomposition Associated with Symmetrical Low-Pass Filter of Example 2

$g_0(n)$	$g_1(n)$	$g_2(n)$
0.2981029	0	0
-0.5416559	0.3454228	0
0.1926081	-0.6480567	0.3145719
0.0448315	0.2497585	-0.5203712
0.008782	0.0631341	0.0854856
-0.0026692	-0.010258	0.1295119
0	0	-0.0066687
0	0	-0.0025295

Table 5: High-Pass Filters Coefficients Satisfying Approximately Shift-Invariant Property with N = 4, K = 2 by Toeplitz Matrix Decomposition Associated with Symmetrical Low-Pass Filter of Example 3

$g_0(n)$	$g_1(n)$	$g_2(n)$
0.3798756	0	0
-0.6048929	0.3722006	0
0.0765551	-0.6016651	0.3861112
0.13613699	0.1030646	-0.6380555
0.0178376	0.1038534	0.1252633
-0.0049140	0.0277976	0.1161225
-0.0005398	-0.004057	0.0126917
-0.0000585	-0.001194	-0.0010162
0	0	-0.0010594
0	0	-0.0000575

Source of support: Nil, Conflict of interest: None Declared